

REGULARIZED SUSCEPTIBILITY TENSOR IMAGING FOR GENERATING WHITE MATTER FIBER COLOR MAPS IN HUMAN BRAIN

Xu Li^{1,2}, Issel Anne L Lim^{1,2}, Craig K Jones^{1,2}, and Peter C.M. van Zijl^{1,2}

¹F.M. Kirby Research Center for Functional Brain Imaging, Kennedy Krieger Institute, Baltimore, Maryland, United States, ²Radiology, Johns Hopkins University School of Medicine, Baltimore, Maryland, United States

TARGET AUDIENCE: Researchers and clinicians working with or interested in quantitative susceptibility mapping or susceptibility tensor imaging.

PURPOSE: High-resolution MR phase/frequency images have shown unique tissue contrast due to tissue magnetic susceptibility effects¹, yet MR phase depends on organ orientation relative to the main magnetic field and holds a nonlocal relationship with the tissue susceptibility distribution.² Quantitative susceptibility mapping (QSM) techniques developed in recent years have made it possible to inversely map the intrinsic tissue susceptibility distribution from MR phase measurements.³⁻⁵ However, recent studies also reflect that MR phase induced by tissue susceptibility depends on the orientation of tissue microstructures, such as white matter fibers, relative to the main magnetic field.⁶ This orientation dependence can be generally described by a second rank susceptibility tensor.⁷⁻¹⁰ Susceptibility tensor imaging (STI) can be used to map white matter in human brain and to track fibers in *ex-vivo* mouse brain.⁷⁻¹⁰ However, proper STI-based fiber mapping in the early work required MR phase measurements collected at a large number of head orientations (>14) which made it quite challenging for human study. In this study we propose some regularization strategies for the STI inverse problem in order to improve the STI performance when data acquisition is limited to small number of head rotations.

METHODS: According to the susceptibility tensor theory, the MR measurable relative magnetic field change $\delta B_z(\vec{r})$ collected at the i th head orientation can be described as in Eqn. (1)^{9,10}. Combining MR phase measurements collected at $N(N \geq 6)$ head orientations in the subject frame of reference,

$$(\delta B_z)_i = \text{FT}^{-1} \left\{ \frac{1}{3} (\hat{H}_0)_i \cdot \text{FT} \{ \bar{\chi} \}_i \cdot (\hat{H}_0)_i - (\hat{H}_0)_i \cdot \bar{k} \cdot \text{FT} \{ \bar{\chi} \} \cdot (\hat{H}_0)_i \right\} \quad (1)$$

STI in principle solves for the 6 tensor components in each imaging voxel. Two regularization strategies are introduced to the STI method. First, for the isotropic voxels, the off-diagonal tensor components vanish i.e. $\chi_{12} = \chi_{13} = \chi_{23} = 0$ and all of the diagonal components equal each other, i.e. $\chi_{11} = \chi_{22} = \chi_{33}$. Second, because the trace of the tensor does not change with respect to the coordinate system, any structural prior information commonly used in QSM regularization, e.g. structure edges, can be applied to regularize the susceptibility tensor trace ($\chi_{11} + \chi_{22} + \chi_{33}$). In order to demonstrate the merit of the proposed method, we compared the imaging performance using STI with and without regularization in both computer simulations and human

studies. The mean magnetic susceptibility (MMS), magnetic susceptibility anisotropy (MSA), and principal eigenvector (PEV) maps of an anisotropic head phantom are shown in Fig. 1. Here, MMS and MSA are defined as $(\chi_{11} + \chi_{22} + \chi_{33})/3$ and $\chi_{11} - 0.5(\chi_{22} + \chi_{33})$ in the tensor diagonal frame of reference, resp. All anisotropic regions in this phantom were set to be cylindrically symmetric. For the simulation study, magnetic field shifts at six head orientations were used, i.e. one normal position, three positions with a rotation angle of 15° and two positions with a rotation angle of 30°. Gaussian noise with an SNR of 30 was added to the field change data. For the *in vivo* human study, phase images were acquired on a normal healthy subject with IRB approval using 3D multi-echo GRE at 7T (1mm isotropic resolution, TR/TE/ΔTE=35/2/2ms, 8 echoes) at six different head orientations with rotation angles of 5°-15°. All data were coregistered in the subject frame.¹⁰ DTI data were collected on the same subjects at 3T (2.2mm isotropic resolution, 32 gradient orientations) and coregistered to the GRE magnitude images for comparison.

RESULTS: Figure 1 shows the simulation results. Compared to the target, the reconstructed MMS and MSA using STI had errors of 14% and 558%, respectively. These were 0.2% and 26% for regularized STI. In addition, when comparing the PEV reconstructions, STI gave a mean angular error of 43.1° in the anisotropic regions, whereas this was 10.8° for regularized STI. Example maps of the reconstructed MMS, MSA, and PEV for human brain are shown in Fig. 2. The reconstructed PEV in white matter is compared to DTI PEV in Fig. 3. The standard STI data are inconclusive for interpretation with this data set, while the regularized STI results show good correspondence of green (anterior-posterior) and red (left-right) components, but not for blue (superior-inferior).

DISCUSSION: The simulations and human data show that the STI method without regularization is quite sensitive to noise and gives large reconstruction errors and spatial variations when the MR phase data is collected at small number of head orientations (6 in this study), while the regularized STI method gives much better performance. Additionally, as compared to STI, the PEV map obtained using the regularized STI method better resembles the PEV map obtained from DTI. However, large differences still exist, especially in fibers around the deep nuclei and fibers oriented in the inferior-superior directions. This may be partly due to the residual background field and the poor inverse condition caused by the restrained head rotation range. Better regularization strategies are needed for STI in the future to make it possible to track all white matter fibers in human brain at a high resolution.

CONCLUSION: The regularized STI method proposed in this study gives better performance than STI without regularization and may facilitate future human STI study with MR phase data collected at a small number of head orientations.

REFERENCES: [1] Duyn JH, et al. PNAS, 2007, 104(28):11796-11801. [2] Salomir R, et al. Concepts Magn. Reson. B, 2003, 19B(1), 26-34. [3] Wharton S, et al. NeuroImage, 2010, 53(2):515-525. [4] Liu T, et al. MRM, 2011, 66(3):777-783. [5] Schweser F, et al. NeuroImage, 2011, 54(4):2789-2807. [6] Lee J, et al. PNAS, 2010, 107(11):5130-5135. [7] Liu C, MRM, 2010, 63(6):1471-1477. [8] Li W, et al. NeuroImage, 2012, 59(3):2088-2097. [9] Liu C, et al. NeuroImage, 2012, 59(2):1290-1298. [10] Li X, et al. NeuroImage, 2012, 62(1):314-330. **Funding:** NIH/NIBIB-P41 EB015909

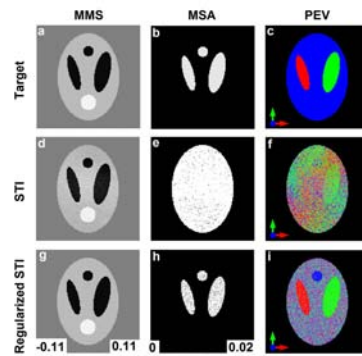


Fig. 1 (a-c) Target MMS, MSA and PEV maps of the head phantom. (d-f) Reconstructed MMS, MSA and PEV maps using STI method with 6 head orientations of 15°-30°. (g-i) Reconstructed MMS, MSA and PEV maps using regularized STI method. Units are ppm.

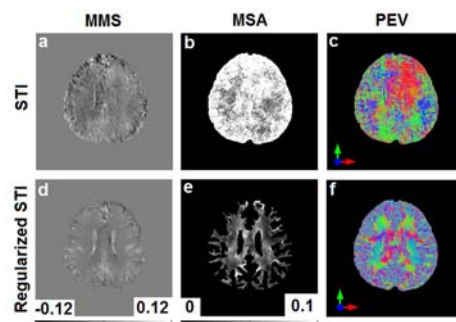


Fig. 2 (a-c) MMS, MSA and PEV maps of a human subject reconstructed using STI method with 6 head orientations. (d-f) MMS, MSA and PEV maps reconstructed using the regularized STI method. All gray scales are in the unit of ppm.

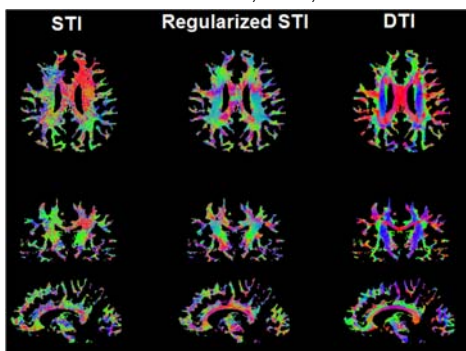


Fig. 3 Comparison of the PEV maps obtained using STI, Regularized STI and DTI in white matter.